

Template Based Rodent Brain Extraction and Atlas Mapping

Weimin Huang, Jiaqi Zhang, Zhiping Lin, Su Huang, Yuping Duan, Zhongkang Lu

Abstract— Accurate rodent brain extraction is the basic step for many translational studies using MR imaging. This paper presents a template based approach with multi-expert refinement to automatic rodent brain extraction. We first build the brain appearance model based on the learning exemplars. Together with the template matching, we encode the rodent brain position into the search space to reliably locate the rodent brain and estimate the rough segmentation. With the initial mask, a level-set segmentation and a mask-based template learning are implemented further to the brain region. The multi-expert fusion is used to generate a new mask. We finally combine the region growing based on the histogram distribution learning to delineate the final brain mask. A high-resolution rodent atlas is used to illustrate that the segmented low resolution anatomic image can be well mapped to the atlas. Tested on a public data set, all brains are located reliably and we achieve the mean Jaccard similarity score at 94.99% for brain segmentation, which is a statistically significant improvement compared to two other rodent brain extraction methods.

I. INTRODUCTION

Magnetic Resonance Imaging (MRI) based rodent imaging is widely used in preclinical study for drug discovery and disease analysis [1]. A structure image such as T2 MRI is often acquired not only for anatomical analysis but also for atlas mapping used together with other functional imaging [2]. As one of the basic steps, accurate rodent brain extraction is critical for the subsequent process and analysis.

Generally speaking, brain extraction is to strip non-brain tissue from an image of the whole head. Automatic methods are widely available for human brain extraction, including region growing [3], edge based [4], atlas based [5] or hybrid method [6]. However human brain extraction methods are not always performing well for rodent/mouse brain images because of the diversities in shapes and differences in intensity variations. There are some methods proposed for rodent/mouse brain extraction. Murugavel and Sullivan [7] proposed a pulse coupled neural network (PCNN) for 2D rodent brain segmentation. As an extension, Chou et al [8] proposed a 3D PCNN method. Li et al. [9] proposed to use the surface model used in brain extraction tool (BET) [3] for rodent data. Uberti et al. proposed a constrained level set for rat brain extraction [10]. Recently, based on layered optimal graph image segmentation, Oguz et al. proposed an automatic method to segment rodent brain [11]. In this paper we propose

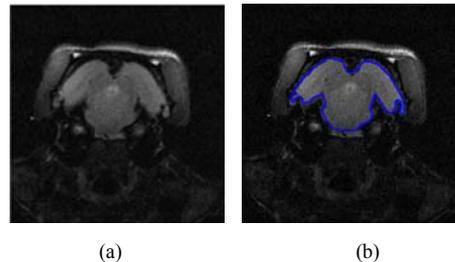


Figure 1. Rodent brain extraction (a) Original head image, (b) Rodent brain label (ground truth).

a template learning based approach to rodent brain extraction from MRI images.

Breitenreicher et al. proposed a sparse template based method to segment occluded and noisy objects [12], with relatively fixed shape model. Mahapatra et al. proposed to use a field of experts and low level image prior model to learn the different tissue features for disease region segmentation [13]. Chen et al. proposed to use template matching approach based on the active appearance model for cell segmentation, which uses training contours chosen by users and deformed by level set method to build a statistical model [14]. Lankton et al. proposed a method that re-formulated the region-based segmentation energy in a local way [16]. The contour of object was evolved based on local information by considering local statistics rather than global one of the images. The results have shown much improvement compared to [15], but still not solving the main challenge in providing the accurate segmentation results affected by leaking to the surrounding structures with the intensity similar to the target objects. Comparatively, example learning is robust to brain extraction. In the multi-instance object segmentation algorithm developed by Chen et al. [17], favorable results on the joint detection and segmentation have been obtained, where the shape prediction through exemplars is incorporated based on Champer-distance of the potential object contours.

In the paper, we propose an approach by exemplar learning and multi-expert refinement for rodent brain extraction in 2D structural MRI images, which has obtained results that are more accurate compared to the (2D/3D) PCNN and modified BET method. We first build the statistic template of the rodent brain using exemplar from training data. The template is used to predict the location of the brain in the head MRI (Fig. 1 shows the original rodent head MRI and the manually labelled brain). Followed by the level set segmentation and mask-based template learning, we take the union of the segments as the region of interest. A slice based histogram distribution learning is then applied to refine the brain region, which can be finally mapped to a high resolution rodent brain atlas.

*Work supported partially by JCO grant 1331AFG077 and JCO DP grant 1334k014, A*STAR, Singapore.

Weimin Huang, Su Huang, Zhongkang Lu are with the Institute for Infocomm Research, 1 Fusionopolis Way, #21-01 Connexis, Singapore 138632, e-mail: {wmhuang, huangs, zklu}@i2r.a-star.edu.sg.

Jiaqi Zhang, Zhiping Lin are with the School of EEE, Nanyang Technological Univ., Singapore, e-mail: {zhan0374, ezplin}@ntu.edu.sg.

Yuping Duan is with Tianjin University, Tianjin, 300072, P.R. China, e-mail: yuping.duan@tju.edu.cn.

II. TEMPLATE BASED RODENT BRAIN EXTRACTION

A. Introduction

Given a set of annotated rodent brain images as exemplars, the template learning is to construct a model for brain extraction on new images. The idea is similar to human brain atlas based segmentation [5]. Different from [5], where K-means clustering technique is used to create the templates from the exemplars, we apply Principle Component Analysis (PCA) [14] to characterize the key variation of the shape of the rodent brains, and use the best template derived from the template model to locate the brain. The shape variation can be extracted from the image warping based on one of the nonlinear image registration methods [14, 24].

The model learnt encodes the main shape and appearance of rodent brain. We can find the maximum of the template matching by scanning across the rodent head image as the brain location. For template learning method, the two main steps are training and segmentation, as shown in Fig. 2. The details will be discussed in the following sections.

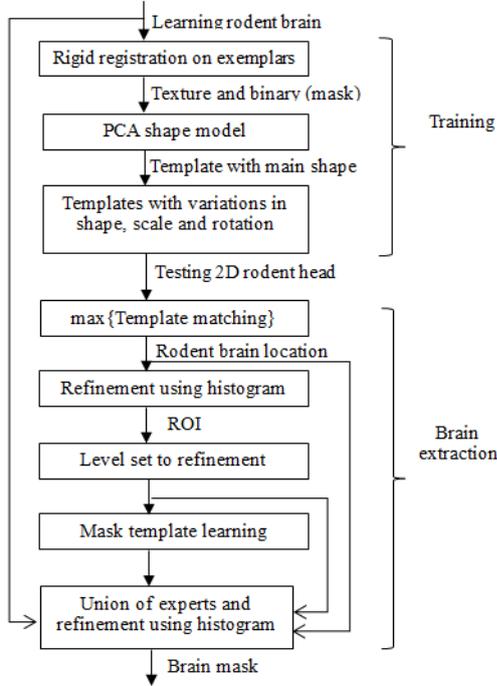


Figure 2. Template training and rodent brain extraction

B. Training templates

Before creating the template, all MRI rodent images are processed by the N4ITK bias correction [18] to reduce the intensity inhomogeneity caused by the MRI process. We focus on 2D brain extraction in this work as quite a lot of preclinical studies only acquire a 2D structural image as navigator. In the future, the 2D extraction method can be extended to 3D model as well.

Let a rodent image at slice k be I^k , with the annotated mask M^k , which is usually manually delineated. The exemplar is E^k , where $E^k = I^k$, if $M^k=I$, else $E^k=0$. For N training exemplars, E_i^k , $i=1, \dots, N$, to construct the template both in the sense of shape and texture. Firstly, every template E_i^k (at one corresponding brain slice) is registered on to a chosen initial

targeted template using rigid transformation function, followed by a nonlinear registration by minimization of the normalized cross correlation (NCC) [14]. The image displacement fields $\{D_i^k=(\Delta X, \Delta Y)\}$ from the nonlinear registration is used to represent the shape variation. By cascading the components in D_i^k into a vector Y_i , the data matrix is written as $\mathbf{D} = [Y_1 - \bar{Y}, Y_2 - \bar{Y}, \dots, Y_N - \bar{Y}]$. $\bar{Y} = \sum Y_i$. The covariance matrix of \mathbf{D} is $\mathbf{A} = \mathbf{D}^T \mathbf{D}$. Applying PCA to \mathbf{D} , we can represent any Y by

$$Y \approx \sum_{k=1}^K \alpha(k) P(k) + \bar{Y},$$

where $P(k)$ is the k -principal component, or the k -th eigenvector of \mathbf{A} , and the $\alpha(k)$ is the coefficient. Usually the top K principal components are selected to cover the 95% of variance of the data. To construct the new templates from the PCA model, we limit the coefficients $\alpha(k)$ by varying it within a range with respect to the eigenvalue thus makes the templates generated using PCA model to embody certain shape varieties. A template (displacement) is defined by

$$T_e = \sum_{k=1}^K \alpha_e(k) P(k) + \bar{Y},$$

where $\alpha_e(k) \in [-C\sqrt{\lambda(k)}, C\sqrt{\lambda(k)}]$, $\lambda(k)$ is the k -th eigenvalue and C is a small constant. By uniformly sampling α_e we can generate new deformation. Applying T_e to the mean of the registered images, we obtained the exemplars. Two examples are shown in Fig. 3. To tackle the changes of brain size and orientation in MRI scanning in different testing sets, additional scaling factor and rotation are applied to generate more templates. The full set of the template is used as the ‘model’ exemplars to locate the rodent brain.

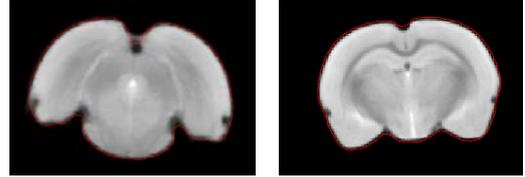


Figure 3. Template examples learnt on different slices

The corresponding binary mask templates can be built in the same process, by using M_k instead of E_k for PCA model.

C. Brain extraction using template learning

Given a testing image I , we compute the similarity between the template and a patch of I . Detection and segmentation is derived based on maximization of the similarity. Each template is seen as a filter denoted as T_t , $t \in [1, \dots, N_T]$, a total of N_T templates. Without loss of generality, we use the NCC measurement as it can be implemented by FFT [20]. The NCC of a model T and image I is:

$$\gamma_T(u) = \frac{\sum_x I(x) T_t(x-u)}{\|I(u)\| \|T_t\|},$$

where u is the position of the patch. As $\|T_t\|$ is a constant, $\|I(u)\|$, the norm of the image patch centered at u , is independent of T_t , the NCC of image I and a set of templates T can be computed efficiently.

Rodent brain detection can be wrong if only using the image similarity. The texture variation between the testing and training data may result in the global maxima being found at other head regions (shown in Fig. 4, right image). Knowing

that rodent brains scanned are always around the center part in the field of view, we encode the head position information by a 2D Gaussian distribution at the mean (x_0, y_0) with standard deviation (σ_x, σ_y) of the mask centers in the training images. The rodent brain location u_l and corresponding template T_l are then found as

$$\{T_l, u_l\} = \max_{u, T} \left\{ \gamma_T(u) \exp \left\{ -\frac{(u_x - x_0)^2}{2\sigma_x^2} - \frac{(u_y - y_0)^2}{2\sigma_y^2} \right\} \right\}.$$

The example results with and without the use of Gaussian distribution is shown in Fig. 4.

D. Refinement by multiple experts

It is sometimes difficult to have the accurate segmentation using pre-learned templates as we have to balance the variability and the robustness [5,19]. The brain location and segmentation is so far robust yet not accurate. Based on the initial brain position and mask from the template learning, we apply the level set method to generate a new mask, which will restore some of the missing parts from the initial template matching. We further apply the (binary) mask template learnt before to the image to generate a new potential brain region.

Refinement is done by learning the histogram distribution for each corresponding slice. Given a region of interest (ROI), i.e. the initial brain region, the histogram distribution is computed by a density estimation method from the pixels in the region. Observing that noisy pixels will be included in the segmentation are often around the boundaries at low intensity, we select a threshold to keep the main distribution between 90%~98%, which is learnt from the training data for a corresponding brain slice. It is applied to the union of the ROIs from template, level set and mask template, followed by morphological operations to remove the small noise.

III. ATLAS MAPPING

The 2D rodent brain extracted can be mapped to a high resolution atlas [21] based on the Waxholm space [22] built on T1-weighted MRI images, using a Bruker 9.4T scanner, image resolution $512 \times 512 \times 512$, at isotropic spatial voxel resolution $59 \mu\text{m}$ [21]. Registration from the 2D structural image to the atlas template is using ANTS [23]. The similarity of an input 2D brain image (Fig. 5(b): yellow contour using the proposed method, red is the ground truth) to the atlas templates (Fig. 5(c)) is shown in Fig. 5, where the possible optimal mapped position is at the atlas slice 280.

IV. EXPERIMENT AND RESULTS

A. Dataset and settings

We test the automatic method on a public available rodent brain data set [7], which has 30 rodent brain volumes, T2 weighted imaging by RARE-pulse-sequence, using Bruker Biospec 4.7Telsa MRI machine, resolution at $256 \times 256 \times 12$ and pixel spacing at $0.12 \text{mm} \times 0.12 \text{mm} \times 1.2 \text{mm}$. Ground truth is manually generated [7].

The proposed brain extraction is tested on the coronal view, image size 256×256 . Totally there are 12 slices per volume. We divide the first 28 volumes into 4 batches, with each batch containing 7 volumes. In cross-validation, each training will use 3 of the 4 batches to build the template model and for histogram-tuning, the other batch will be used as testing data. The volume 29 and 30 will be used only in testing

(with batch 1). Training and testing is slice-based. The additional scale change of the template is starting from 0.9 to 1.1, with increase of 0.1 each step. The orientation is from $-\pi/30$ to $+\pi/30$, with interval $\pi/60$. The variation of the PCA coefficient is constrained by $2\sqrt{\lambda}$.

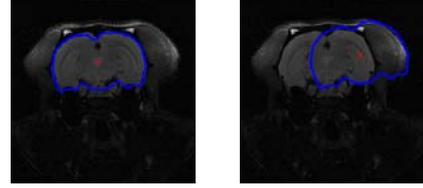
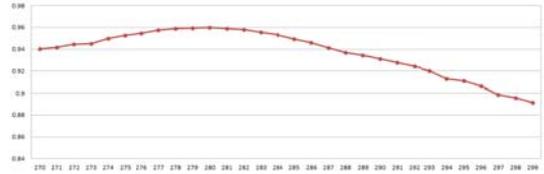


Figure 4. Template matching results with and without the use of Gaussian distribution of brain mask.



(a) Similarity between atlas template (T1 weighted) and the brain extracted (T2 weighted) using ANTS registration for atlas mapping.

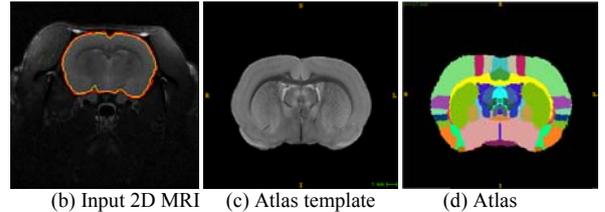


Figure 5. Atlas registration similarity chart. Input image and the atlas template.

The Jaccard similarity (J -score) is used to measure the performance of the rodent brain extraction [7]. It is defined as

$$J = \frac{M \cap G}{M \cup G},$$

where M is the result generated by a method and G is the ground truth. When the whole volume is used to compute the J -score of rodent brain, we call it volume J -score.

B. Experiment Result

The mean J -score of our method is 94.99%. Fig. 6 shows some of the detection results: (a) Initial brain by applying template learning; (b) Result using level set; (c) Result using mask template learning; (d) Final result by combination of the masks and the histogram tuning, where the red line is the ground truth and the yellow line is from our method. The red cross in Fig. 6(a) is the detected brain center.

For the template based brain extraction we achieve $J=91.97\%$, with minimum $J=78.03\%$, which means we can always locate the main brain from the head MRI. Using neighboring slice model will not affect the brain location too much. Compared to our result of mean $J=94.99\%$, the mean J -score by 2D PCNN is 0.93 [7]. Fig. 7(a) is the boxplot of the volume J -score compared to 3D PCNN [8] and BET [3], all based on N4 [18] bias removed data. It shows that the proposed method achieves better extraction accuracy. The

t-test manifests that the improvement is statistically significant with $p < 0.001$ compared to 3DPCNN result and $p < 0.0001$ compared to BET. The individual boxplot from the proposed method for the 12 slices and 30 volumes are also shown in Fig. 7(b) and (c). The overall performance for different slices is different. Usually, the smoother of the boundary of the brain, the better the method can achieve for the brain segmentation.

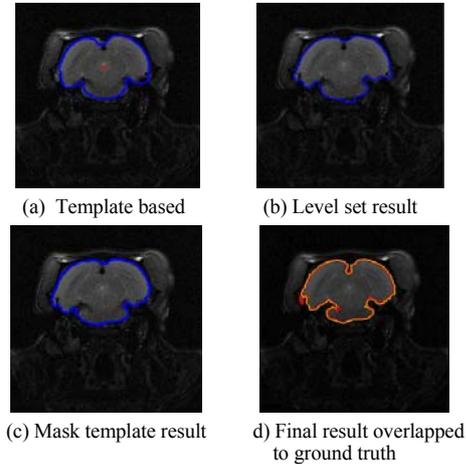


Figure 6. Segmentation procedure and stage Results

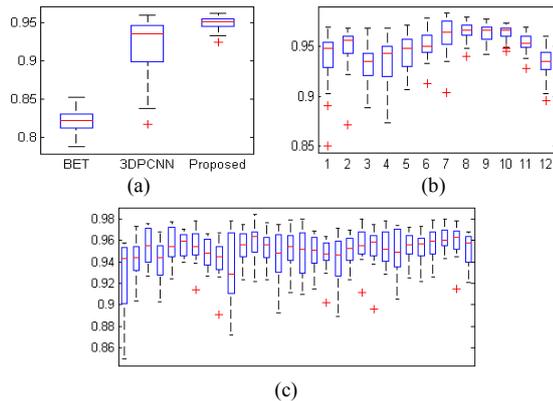


Figure 7. Comparison of the brain extraction. (a) Volume J -score of different methods, (b) slice J -score at the 12 different slices of the dataset, (c) slice J -score for each rat volume

V. CONCLUSION

We have proposed a template based method to extract the rodent brain in T2 weighted MRI images. We achieved results with accuracy significantly higher than the compared methods. The results suggest that the learning based method has the potential to identify and segment the main structures from anatomical images. Using the cropped brain, we demonstrated that it was possible to register the image navigator to a high resolution atlas. More dataset can be tested in the future and further research can be done to incorporate the local intensity and context feature to improve the extraction accuracy.

REFERENCES

- [1] D. Van Dam and P. P. De Deyn, "Drug discovery in dementia: the role of rodent models," *Nature Reviews Drug Discovery*, vol. 5, no. 11, pp. 956–970, 2006.

- [2] W. Cui et al., "Non-invasive measurement of cerebral oxygen metabolism in the mouse brain by ultra-high field 17O MR spectroscopy," *Journal of Cerebral Blood Flow & Metabolism*, vol. 33, pp.1846–1849, 2013.
- [3] S. M. Smith, "Fast robust automated brain extraction," *Human Brain Mapping*, vol. 17, no. 3, pp. 143–155, 2002.
- [4] D. W. Shattuck and R. M. Leahy, "Brainsuite: an automated cortical surface identification tool," *Medical Image Analysis*, vol. 6, no. 2, pp. 129–142, 2002.
- [5] J. Doshi et al., "Multi-Atlas Skull-Stripping," *Academic Radiology*, vol. 20, no 12, pp. 1566–1576, 2013.
- [6] F. S'egonne, et al., "A hybrid approach to the skull stripping problem in mri," *Neuroimage*, vol. 22, no. 3, pp. 1060–1075, 2004.
- [7] M. Murugavel and J. Jr., "Automatic Cropping of MRI Rat Brain Volumes using Pulse Coupled Neural Networks," *NeuroImage*, vol. 45, no 3, pp.845-854, 2008.
- [8] N. Chou, J. Wu, J. B. Bingren, A. Qiu, and K. Chuang, "Robust Automatic Rodent Brain Extraction Using 3-D Pulse-Coupled Neural Networks (PCNN)," *IEEE Transactions on Image Processing*, vol. 20, no. 9, pp.2554-2564, 2011.
- [9] J. Li, X. Liu, J. Zhuo, R. P. Gullapalli, and J. M. Zara, "An automatic rat brain extraction method based on a deformable surface model," *Journal of Neuroscience Methods*, vol. 218, no. 1, pp. 72–82, 2013.
- [10] M. G. Uberti, M. D. Boska, and Y. Liu, "A semi-automatic image segmentation method for extraction of brain volume from in vivo mouse head magnetic resonance imaging using constraint level sets," *J. of Neuroscience Methods*, vol. 179, no. 2, pp. 338–344, 2009.
- [11] I. Oguz, H. Zhang, A. Rumble, and M. Sonka, "Rats: rapid automatic tissue segmentation in rodent brain mri," *J. of Neuroscience Methods*, vol. 221, pp. 175–182, 2014.
- [12] D. Breitenreicher, J. Lellmann and C. Schnorr, "Sparse Template-Based Variational Image Segmentation," *Advances in Adaptive Data Analysis*, vol. 3 no. 1-2, pp. 149-166, 2011.
- [13] D. Mahapatra, P. Schüffler, F. Vos, J. M. Buhmann, "Crohn's disease segmentation from MRI using learned image priors," *IEEE ISBI'15*, pp. 625-628, 2015.
- [14] C. Chen, W. Wang, J. Ozolek, G. Rohde, "A flexible and robust approach for segmenting cell nuclei from 2D microscopy images using supervised learning and template matching," *Cytometry a*, pp. 495-507, 2013
- [15] K. Zhang, L. Zhang, H. Song, W. Zhou, "Active contours with selective local or global segmentation: A new formulation and level set method," *Image and Vision Computing*, vol. 28, pp.668–676, 2010.
- [16] S. Lankton, A. Tannenbaum, "Localizing Region-Based Active Contours," *IEEE Trans Image Process.*, vol. 17, no. 11, pp. 2029-2039, 2009.
- [17] Y. Chen, X. Liu, M. Yang, "Multi-instance Object Segmentation with Occlusion Handling," *IEEE Conf on Computer Vision and Pattern Recognition*, pp. 3470 – 3478, 2015
- [18] N. J. Tustison et al., "N4ITK: Improved N3 bias correction," *IEEE Trans. Medical Imaging*, vol. 29, no. 6, pp. 1310–1320, 2010.
- [19] G. Sanroma, G. Wu, Y. Gao, D. Shen, "Learning-Based Atlas Selection for Multiple-Atlas Segmentation," *IEEE CVPR'14*, pp. 3111-3117, 2014.
- [20] K. Briechle and U. D. Hanebeck, "Template matching using fast normalized cross correlation", *Proc. SPIE 4387, Optical Pattern Recognition XII*, 95, 2001.
- [21] S. Huang et al., "High Resolution in vivo Wistar Rodent Brain Atlas based on T1 weighted Image," *Proc. SPIE Medical imaging*, 2016.
- [22] G.A. Johnson, A. Badea, J. Brandenburg et al, "Waxholm space: an image-based reference for coordinating mouse brain research," *Neuroimage*, vol. 53, no. 2, pp.365-72, 2010.
- [23] B. B. Avants, C. L. Epstein, M. Grossman M, J.C. Gee, "Symmetric diffeomorphic image registration with cross-correlation: evaluating automated labeling of elderly and neurodegenerative brain," *Med Image Anal.*, vol. 12, no. 1, pp. 26-41, 2008.
- [24] D. Rueckert and J.A. Schnabel, "Medical image registration," In: *Biomedical Image Processing (TM Deserno, Ed.)*, Series on Biological and Medical Physics, Biomedical Engineering, Springer, 2011.